Aluminum-27 and C-13 NMR Studies of Aluminum (3+) Binding to Ovotransferrin and Its Half-Molecules

ARTICLE *in* JOURNAL OF THE AMERICAN CHEMICAL SOCIETY · JANUARY 1994

Impact Factor: 12.11 · DOI: 10.1021/ja00054a035

2 AUTHORS:

James M Aramini
City University of New York - Advanced Scien…
99 PUBLICATIONS **2,630** CITATIONS
SEE PROFILE

Hans J Vogel
The University of Calgary
417 PUBLICATIONS **14,255** CITATIONS
SEE PROFILE

Aluminum-27 and Carbon-13 NMR Studies of Aluminum(3+) Binding to Ovotransferrin and Its Half-Molecules

James M. Aramini and Hans J. Vogel*

Contribution from the Division of Biochemistry, Department of Biological Sciences, University of Calgary, Calgary, Alberta, Canada T2N 1N4. *Received June 24, 1992*

Abstract: The binding of Al^{3+} to ovotransferrin and its half-molecules in the presence of ^{13}C-enriched carbonate and oxalate has been investigated by ^{27}Al and ^{13}C NMR spectroscopy. With carbonate as the synergistic anion, two overlapping signals are observed in both the ^{13}C and ^{27}Al NMR spectra; these correspond to the chelated Al^{3+} and the labeled anion at both metal ion binding sites in the protein. In the case of oxalate and Al^{3+} binding, two closely spaced ^{27}Al signals are also observed. Two pairs of doublets are detected in the ^{13}C NMR spectrum, suggesting that oxalate binds via only one carboxylate moiety to the metal ion in each site. The chemical shifts of the protein-bound ^{27}Al signals are diagnostic of octahedrally coordinated aluminum. ^{13}C and ^{27}Al NMR experiments on the purified N- and C-terminal half-molecules of ovotransferrin have facilitated the assignment of these signals. From these assignments and titration experiments we found that in the presence of carbonate the N-terminal site of ovotransferrin binds Al^{3+} with a higher affinity than does the C-site. However, changing the synergistic anion to oxalate alters the specificity; under these conditions Al^{3+} is preferentially complexed by the C-site of the protein. These experiments demonstrate a clear difference in the behavior of the two metal ion binding sites of ovotransferrin. The ovotransferrin-bound ^{27}Al NMR signals have some rather unusual properties characteristic of quadrupolar nuclei bound in slow exchange to large macromolecules far from extreme narrowing conditions. First, the maximum intensity of the protein-bound ^{27}Al signal is substantially less than that observed for equimolar solutions of the free metal ion. Second, the signals exhibit a unique pulse angle dependence where a maximum in peak intensity is attained at pulse lengths that are less than half the 90° pulse for an aqueous Al^{3+} solution. Third, ^{27}Al signals for Al^{3+} bound to the half-molecules of ovotransferrin are much broader than those for the intact protein, reflecting the importance of molecular motion on the detectability of quadrupolar nuclei. Fourth, an increase in the external magnetic field strength causes line narrowing and a 2-4 ppm downfield dynamic frequency shift. These data are all consistent with the idea that only the central ($^1/_2 \rightarrow -^1/_2$) transition of the ^{27}Al (spin $^5/_2$) nucleus is observed. This ^{27}Al NMR study exemplifies the potential of this nucleus as a probe for the nature of the iron binding sites of transferrins and possibly other metalloproteins.

Introduction

Transferrins are a class of large (MW ≈ 80 kDa) nonheme iron-binding glycoproteins that are of major physiological importance in vertebrates. Three main types of transferrins have been characterized: serotransferrin (sTf),[1] a key serum protein which serves as a shuttle for metabolic iron, ovotransferrin (OTf), present in avian egg white, and lactoferrin (lTf), found primarily in milk. The latter two provide defense against bacterial infection. An understanding of the structure and function of transferrins has been the object of extensive research, and several comprehensive reviews on the subject have appeared in the literature over the last decade.[2-7]

Transferrins are bilobal molecules, each lobe containing one high-affinity Fe^{3+} binding site ($K_D \leq 10^{-20}$ M). Metal ion binding in both sites is accompanied by the binding of an anion (in vivo, (bi)carbonate). The participation of a "synergistic" anion in the metal binding process is a unique aspect of transferrin chemistry. In addition to ferric ion, transferrins may chelate a broad spectrum of other metal ions varying in both charge and size. As a result, metal ion binding to transferrins has been investigated by a variety of spectroscopic tools, including NMR spectroscopy. ^{13}C NMR studies[8-11] on a number of metal ion derivatives of sTf and OTf in the presence of isotopically enriched anions (either carbonate or oxalate) have provided strong evidence in favor of the direct binding of the anion to the metal ion in each site (consistent with the so-called interlocking sites model[12]). In addition, studies involving the direct detection of a number of diamagnetic metal ions in place of the paramagnetic ferric ion (i.e., using ^{113}Cd, ^{51}V, and ^{205}Tl NMR spectroscopy[8,13-16]) have uncovered subtle differences between the iron binding sites in both sTf and OTf. The recent X-ray crystal structure of human lTf has shed considerable light on the nature of the metal binding sites in transferrins.[17,18] In each site, Fe^{3+} is complexed to four highly conserved protein residues—one aspartate, one histidine, and two tyrosines.[19] The octahedral coordination sphere of the metal ion is completed by carbonate, which appears to be bound in a bidentate fashion to Fe^{3+} and also lies in close proximity to a number of conserved positively charged moieties in each binding site. Virtually identical structures have been reported for rabbit sTf and its N-terminal half-molecule.[20,21] Due to the significant amount of homology

* To whom correspondence should be addressed.

(1) Abbreviations used: NMR, nuclear magnetic resonance; sTf, serotransferrin; OTf, ovotransferrin; lTf, lactoferrin; Fe_2OTf, diferric ovotransferrin; OTf/2N, N(amino)-terminal half-molecule of ovotransferrin; OTf/2C, C(carboxyl)-terminal half-molecule of ovotransferrin; TPCK, L-1-tosylamido-2-phenylethyl chloromethyl ketone; PAS, periodate-Schiff; FID, free-induction decay; TMS, tetramethylsilane; sTf/2N, N(amino)-terminal half-molecule of serotransferrin.

(2) Crichton, R. R. *Adv. Protein Chem.* **1990**, *40*, 281-363.
(3) Aisen, P. In *Physical Bioinorganic Chemistry*; Loehr, T. M., Ed.; VCH Publishers: New York, 1989; Vol. 5, pp 353-371.
(4) Crichton, R. R.; Charloteaux-Wauters, M. *Eur. J. Biochem.* **1987**, *164*, 485-506.
(5) Heubers, H. A.; Finch, C. A. *Physiol. Rev.* **1987**, *67*, 520-582.
(6) Brock, J. H. In *Metalloproteins*; Harrison, P. M., Ed.; MacMillan Press: London, 1985; Part 2, pp 183-262.
(7) Chasteen, N. D. *Adv. Inorg. Biochem.* **1983**, *5*, 201-233.
(8) Sola, M. *Inorg. Chem.* **1990**, *29*, 1113-1116.
(9) Bertini, I.; Messori, L.; Pellacani, G. C.; Sola, M. *Inorg. Chem.* **1988**, *27*, 761-762.
(10) Bertini, I.; Luchinat, C.; Messori, L.; Scozzafava, A.; Pellacani, G.; Sola, M. *Inorg. Chem.* **1986**, *25*, 1782-1786.
(11) Zweier, J. L.; Wooten, J. B.; Cohen, J. S. *Biochemistry* **1981**, *20*, 3505-3510.
(12) Schlabach, M. R.; Bates, G. W. *J. Biol. Chem.* **1975**, *250*, 2182-2188.
(13) Sola, M. *Eur. J. Biochem.* **1990**, *194*, 349-353.
(14) Butler, A.; Eckert, H. *J. Am. Chem. Soc.* **1989**, *111*, 2802-2809.
(15) Butler, A.; Danzitz, M. J.; Eckert, H. *J. Am. Chem. Soc.* **1987**, *109*, 1864-1865.
(16) Bertini, I.; Luchinat, C.; Messori, L. *J. Am. Chem. Soc.* **1983**, *105*, 1347-1350.
(17) Anderson, B. F.; Baker, H. M.; Norris, G. E.; Rice, D. W.; Baker, E. N. *J. Mol. Biol.* **1989**, *209*, 711-734.
(18) Anderson, B. F.; Baker, H. M.; Dodson, E. J.; Norris, G. E.; Rumball, S. V.; Waters, J. M.; Baker, E. N. *Proc. Natl. Acad. Sci. USA* **1987**, *84*, 1769-1773.
(19) The exact residues involved in Fe^{3+} binding in lTf are as follows (C-site in parentheses): Asp-60 (395), Tyr-92 (435), Tyr-192 (528), His-253 (597). Several positively charged groups, including the side chain of Arg-121 (465) and the N-terminus of an α-helix, are juxtaposed to the bound anion.
(20) Bailey, S.; Evans, R. W.; Garratt, R. C.; Gorinsky, B.; Hasnain, S.; Horsburgh, C.; Jhoti, H.; Lindley, P. F.; Mydin, A.; Sarra, R.; Watson, J. L. *Biochemistry* **1988**, *27*, 5804-5812.

0002-7863/93/1515-245$04.00/0

in the amino acid sequences of the transferrins,[22] a similar picture is expected for OTf, although a high-resolution X-ray study of this protein has not been reported to date.

In vivo, transferrins are thought to be only partially saturated with ferric ion (≈30%), and this, together with their propensity for binding a variety of metal ions, has fueled speculation regarding a possible role for these proteins in the chelation and removal of toxic metal ions such as Al^{3+}. Although aluminum has no known biological function, a toxic amount of Al^{3+} can cause dialysis encephalopathy in humans and is associated with other degenerative disorders such as senile dementia of the Alzheimer's type.[23] Recent evidence suggests that sTf from people afflicted with Alzheimer's disease may be deficient in its ability to complex and remove Al^{3+}, contributing to the deposition of high levels of this metal in the brain.[24] Of late, the binding of Al^{3+} to transferrins has been probed by a number of spectroscopic techniques,[10,25-27] underscoring the growing interest in the medically relevant aluminum derivatives of these proteins.

In this paper we present a high-field ^{27}Al and ^{13}C NMR study of Al^{3+} binding to OTf and the half-molecules of this protein. ^{27}Al has a quadrupolar ($I = {}^5/_2$) nucleus which possesses a number of favorable traits (i.e., a good receptivity and high natural abundance) that make it amenable to study by NMR.[28,29] However, ^{27}Al NMR has been used as a spectroscopic marker for the binding of Al^{3+} to proteins only once prior to this report.[30]

Experimental Section

Materials. Apo-ovotransferrin and diferric ovotransferrin from chicken egg white were purchased from Sigma Chemical Co. The apoprotein was rendered free of low molecular weight impurities by dialysis against 0.10 M $NaClO_4$, followed by exhaustive dialysis against double-distilled water.[31] The N- and C-terminal half-molecules of ovotransferrin were obtained by digestion of Fe_2OTf with TPCK-treated bovine pancreatic trypsin (Sigma Chemical Co.) and purified according to a previously published method.[32] The isolated half-molecules were assigned using a sensitive PAS assay for glycoproteins[33] on the basis of the fact that only OTf/2C is glycosylated.[2,34] In order to regenerate the apo forms of both half-molecules upon completion of an experiment, used OTf/2N and OTf/2C samples were dialyzed against 0.10 M sodium citrate, pH 4.5, and repeatedly against double-distilled water. All protein samples were lyophilized and stored at −20 °C prior to use.

Ultrapure aluminum nitrate and potassium chloride were purchased from Aldrich Chemical Co. The sodium salts of ^{13}C-enriched (99%) carbonate and oxalate, $Na_2{}^{13}CO_3$ and $Na_2{}^{13}C_2O_4$, were obtained from MSD Isotopes. Deuterium oxide (99.9%) was obtained from Cambridge Isotope Laboratories. All other chemicals used in this work were of the highest quality available.

NMR Spectroscopy. NMR samples were prepared by dissolving the lyophilized proteins in 1.8–2.0 mL of double-distilled water containing 25% v/v D_2O (lock), 150 mM KCl, and 2.5–20 mM $Na_2{}^{13}CO_3$ or $Na_2{}^{13}C_2O_4$. Apo-OTf concentrations were determined by absorption at λ = 280 nm on a Cary 1 UV–visible spectrophotometer using a molar extinction coefficient (ϵ_{280}) of 91 200 M^{-1} cm^{-1}. Half-molecule concentrations were deduced from the weight of each lyophilized sample using literature values for their respective molecular weights.[32] For each protein sample, Al^{3+} titrations were performed by adding microliter amounts of an aqueous $Al(NO_3)_3$ stock solution, and the pH was adjusted to the desired value by microliter additions of 1.0 M KOD and 1.0 M DCl. All pH values shown were measured with a 3.5-mm calomel electrode (Ingold Electronics) using a Fisher Accumet 805MP pH meter.

^{27}Al and proton-coupled ^{13}C NMR spectra were recorded on a wide-bore Bruker AM-400 spectrometer equipped with a 10-mm broadband probe at resonance frequencies of 104.3 and 100.6 MHz for ^{27}Al and ^{13}C, respectively. ^{27}Al NMR spectra were also obtained at a frequency of 130.3 MHz on a Bruker AMX-500 instrument equipped with a 10-mm broadband probe. All spectra were recorded locked and at 25 °C. ^{27}Al NMR spectra were acquired with the following parameters: a 45° pulse length (10–18 μs depending on the spectrometer), 50–250 ms between pulses, a sweep width of 50 000 Hz, and a spectrometer dead time of 240 μs.[35] Each FID was zero-filled to 16K, and an exponential multiplication resulting in a line broadening of 20 Hz was applied prior to Fourier transformation. A simulation program (LINESIM, written by P. Barron, Bruker, Australia) was used to determine chemical shifts, line widths, and relative areas of overlapping ^{27}Al signals. All ^{27}Al NMR spectra are referenced to external 1.0 M $Al(NO_3)_3$ in D_2O. Typical ^{13}C NMR acquisition parameters used in this study are as follows: a 5.6-μs (50°) pulse length, a 2.1-s repetition time, and a sweep width of 25 000 Hz. Again, a line broadening (7 Hz) was applied to all ^{13}C data prior to processing. All ^{13}C NMR spectra are referenced to internal dioxane (δ = 67.40 with respect to TMS).

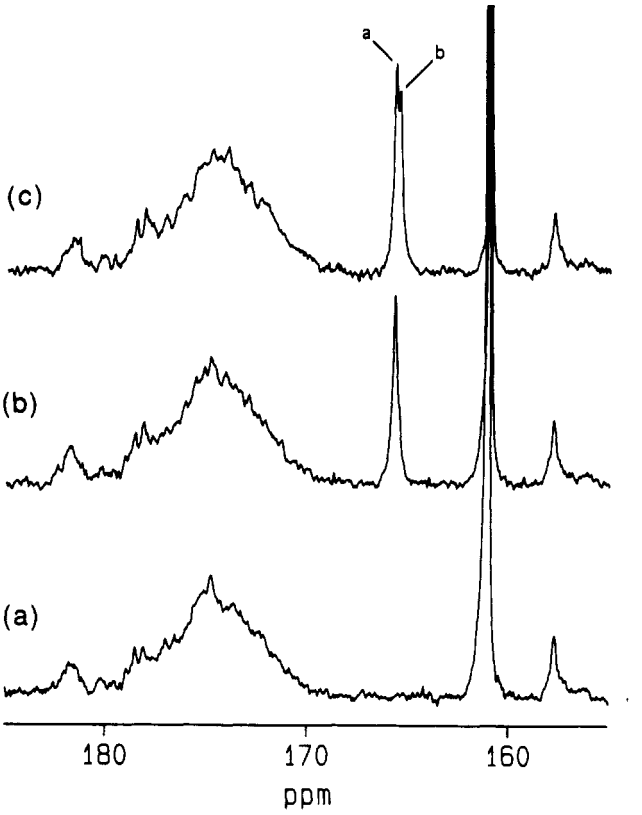

Figure 1. ^{13}C NMR spectra (100.6 MHz) of 1.13 mM OTf in the presence of 20 mM $Na_2{}^{13}CO_3$ and various amounts of Al^{3+} (pH 7.6, 20 000 scans each). (a) 0 equiv of Al^{3+}; (b) 1.0 equiv of Al^{3+}; (c) 2.0 equiv of Al^{3+}. Only the carbonyl region of each spectrum is shown.

Results

Experiments with Carbonate as the Synergistic Anion. Proton-coupled ^{13}C NMR spectra of the binding of Al^{3+} to apo-ovotransferrin in the presence of excess ^{13}C-enriched carbonate

(21) Sarra, R.; Garratt, R.; Gorinsky, B.; Jhoti, H.; Lindley, P. *Acta Crystallogr.* **1990**, *B46*, 763–771.
(22) Metz-Boutique, M.-H.; Jollès, J.; Mazurier, J.; Schoentgen, F.; Legrand, D.; Montreuil, J.; Jollès, P. *Eur. J. Biochem.* **1984**, *145*, 659–676.
(23) See articles in the following: *Metal Ions in Biological Systems*; Sigel, H., Ed.; Marcel Dekker: New York, 1988; Vol. 24.
(24) Farrar, G.; Altmann, P.; Welch, S.; Wychrij, O.; Ghose, B.; Lejeune, J.; Corbett, J.; Prasher, V.; Blair, J. A. *Lancet* **1990**, *335*, 747–750.
(25) Kubal, G.; Sadler, P. J. *J. Am. Chem. Soc.* **1992**, *114*, 1117–1118.
(26) Harris, W. R.; Sheldon, J. *Inorg. Chem.* **1990**, *29*, 119–124.
(27) Ichimura, K.; Kihara, H.; Yamamura, T.; Satake, K. *J. Biochem.* (*Tokyo*) **1989**, *106*, 50–54.
(28) Akitt, J. W. *Prog. Nucl. Magn. Reson. Spectrosc.* **1989**, *21*, 1–149.
(29) Delpuech, J. J. In *NMR of Newly Accessible Nuclei*; Laszlo, P., Ed.; Academic Press: New York, 1983; Vol. 2, pp 153–195.
(30) Fatemi, S. J. A.; Williamson, D. J.; Moore, G. R. *J. Inorg. Biochem.* **1992**, *46*, 35–40.
(31) Chasteen, N. D.; Grady, J. K.; Holloway, C. E. *Inorg. Chem.* **1986**, *25*, 2754–2760.
(32) Oe, H.; Doi, E.; Hirose, M. *J. Biochem.* (*Tokyo*) **1988**, *103*, 1066–1072.
(33) Thornton, D. J.; Holmes, D. F.; Sheehan, J. K.; Carlstedt, I. *Anal. Biochem.* **1989**, *182*, 160–164.
(34) OTf contains a single glycan attached to an asparagine at position 473: Williams, J.; Elleman, T. C.; Kingston, I. B.; Wilkins, A. G.; Kuhn, K. A. *Eur. J. Biochem.* **1982**, *122*, 297–303. Dorland, L.; Haverkamp, J.; Vliegenthart, J. F. G.; Spik, G.; Fournet, B.; Montreuil, J. *Eur. J. Biochem.* **1979**, *100*, 569–574.

(35) This value for the dead time is required to effectively attenuate a very broad ($\Delta\nu_{1/2} \approx 7$ kHz) resonance due to aluminum in the materials used to construct the probe (see ref 28 herein). Spectra acquired with much shorter dead times showed no appreciable difference in signal intensity or additional broad resonances.

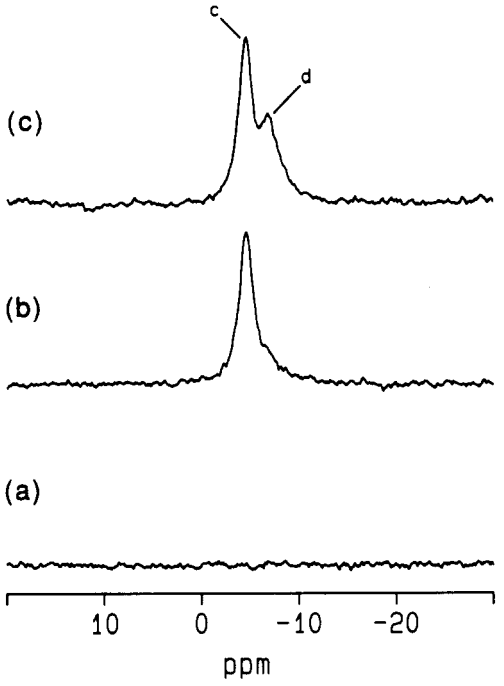

Figure 2. ^{27}Al NMR spectra (104.3 MHz) of 1.13 mM OTf in the presence of 20 mM $Na_2{}^{13}CO_3$ and various amounts of Al^{3+} (pH 7.6, 150 000 scans each): (a) 0 equiv of Al^{3+}; (b) 1.0 equiv of Al^{3+}; (c) 2.0 equiv of Al^{3+}.

are shown in Figure 1. In the absence of Al^{3+} one observes in the carbonyl region of the spectrum a sharp signal at $\delta = 161.1$ due to the labeled anion (primarily bicarbonate at this pH) plus natural abundance ^{13}C resonances corresponding to backbone and side-chain carbonyls ($\delta \approx 170$–183) and the guanidinium group of arginine residues ($\delta = 157.8$) in the protein (Figure 1a). When 1 equiv of Al^{3+} is added to the protein solution, a signal (peak a) emerges at $\delta = 165.73$, in a region devoid of peaks for the apoprotein. A second signal (b) appears at $\delta = 165.52$ upon addition of a second equivalent of the metal ion. The overlapping signals correspond to carbonate[36] bound in a ternary complex with Al^{3+} and OTf in each of the two iron binding sites of this protein. An analogous picture is obtained when one monitors the same experiment using ^{27}Al NMR (Figure 2). A broad resonance (peak c) appears at $\delta = -4.6$ ($\Delta\nu_{1/2} = 180$ Hz) after the first equivalent of Al^{3+}, followed by the emergence of a signal (d) in close proximity to the first ($\delta = -6.8$, $\Delta\nu_{1/2} = 240$ Hz) upon addition of a second equivalent of the metal ion.[37] The ^{13}C and ^{27}Al NMR results clearly indicate that in the presence of carbonate one site of ovotransferrin has a much higher affinity for Al^{3+} than the other, since the signals diagnostic of Al^{3+} binding appear sequentially as the metal ion is added to the protein. Using the areas of peaks a–d, curves for the complete titration of ovotransferrin with Al^{3+} in the presence of $^{13}CO_3{}^{2-}$ have been determined (Figure 3). Both the ^{13}C and ^{27}Al signal areas increase linearly with the addition of up to 1 equiv of metal ion. However, the titration curve wanes with the addition of more metal ion, until there is no further increase in signal area at Al^{3+} levels in excess of 2 equiv. The protein is only ≈85% saturated with metal ion at the completion of the titration. From simulations of the overlapping ^{27}Al signals shown in Figure 2c, the area of peak d is only ≈70% of peak c after 2 equiv of Al^{3+} are added to OTf under these conditions, meaning that complete saturation of the second (weaker) site is not accomplished.

(36) On the basis of ^{13}C chemical shift and pH data and the recent refined X-ray structures of lTf and rabbit sTf/2N, it is widely believed that carbonate (not bicarbonate) serves as the synergistic anion in transferrins (see refs 10, 11, 17, and 21 herein); hence in the text we refer to carbonate as the form of the bound anion.

(37) Similar results were obtained in the absence of salt, in the presence of 150 mM NaCl, and when unpurified OTf was used.

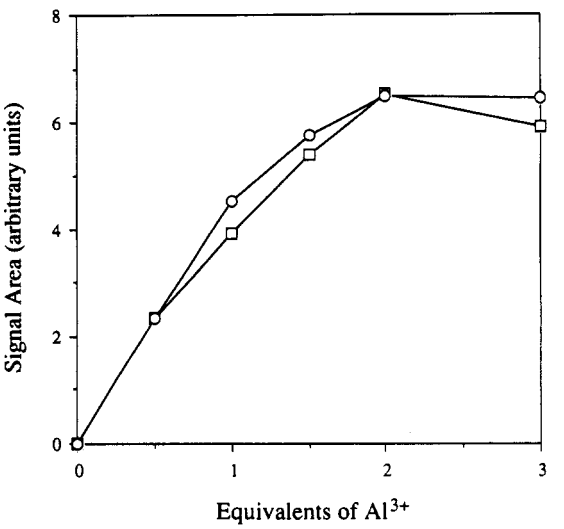

Figure 3. Dependence of the integrated signal areas of the ^{13}C (□) and ^{27}Al (○) NMR resonances corresponding to the binding of Al^{3+} to apo-OTf (1.13 mM, pH 7.6) in the presence of ^{13}C-labeled carbonate (20 mM) on the amount of metal ion added to the protein solution. At each point in the titration, both a ^{13}C and a ^{27}Al NMR spectrum were acquired (20 000 and 150 000 scans, respectively).

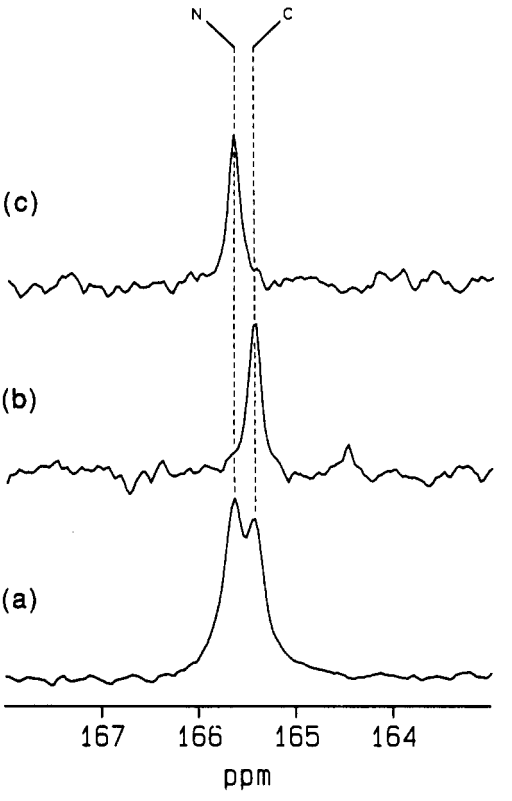

Figure 4. ^{13}C NMR spectra (100.6 MHz) of the aluminum carbonate derivatives of intact OTf and its half-molecules: (a) 1.13 mM OTf, 20 mM $Na_2{}^{13}CO_3$, 2 equiv of Al^{3+}, pH 7.6, 20 000 scans; (b) 1.25 mM OTf/2C, 10 mM $Na_2{}^{13}CO_3$, 1 equiv of Al^{3+}, pH 7.8, 20 000 scans; (c) 0.19 mM OTf/2N, 5 mM $Na_2{}^{13}CO_3$, 1 equiv of Al^{3+}, pH 7.7, 60 000 scans. Only a narrow window of the carbonyl region of each spectrum is shown.

The assignment of the ^{13}C and ^{27}Al NMR signals resulting from Al^{3+} and $^{13}CO_3{}^{2-}$ binding to ovotransferrin (peaks a–d) has been obtained by analyzing the isolated N- and C-terminal half-molecules of the protein. ^{13}C NMR spectra of the aluminum carbonate derivatives of OTf, OTf/2C, and OTf/2N are shown in Figure 4. To facilitate a direct comparison between the three molecules, expansions of the carbonyl region of each spectrum including only the relevant signals are shown. Again, for the intact

Table I. ^{13}C and ^{27}Al NMR Data for the Binding of Al^{3+} to OTf, OTf/2N, and OTf/2C in the Presence of ^{13}C-Labeled Carbonate[a]

(a) ^{13}C NMR

peak	δ	assignment[b]
a	165.73	N-site
b	165.52	C-site

(b) ^{27}Al NMR

peak	δ	$\Delta\nu_{1/2}$ (Hz)	assignment[b]
c	−4.6	180	N-site
	(−2.3)	(140)	N-site
d	−6.8	240	C-site
	(−3.8)	(170)	C-site
OTf/2N	−4.6	410	
OTf/2C	−6.5	460	

[a] All ^{13}C data were acquired at a frequency of 100.6 MHz (9.4 T). The ^{27}Al data shown were obtained at frequencies of 104.3 MHz (9.4 T) and 130.3 MHz (11.7 T, in parentheses). [b] From ^{13}C NMR experiments on OTf/2N and OTf/2C; the ^{27}Al NMR assignments are also supported by the ^{27}Al chemical shifts for the half-molecules.

protein two overlapping resonances are observed, corresponding to the binding of carbonate to each metal ion binding site in OTf (Figure 4a). When a stoichiometric amount of Al^{3+} is added to OTf/2C in the presence of the same anion, a signal appears at exactly the same chemical shift as peak b in the intact molecule (Figure 4b). In the case of OTf/2N, only the downfield resonance (a) is observed (Figure 4c). A complete list of the ^{13}C and ^{27}Al NMR signals diagnostic of Al^{3+} and $^{13}CO_3^{2-}$ binding to ovotransferrin and their assignments is presented in Table I. Taken together with the results shown in Figures 1 and 2, the half-molecule experiments indicate that in the presence of carbonate the N-terminal site of OTf has a higher affinity for Al^{3+} than does the C-site. Of note is the fact that ^{27}Al NMR signals for the aluminum carbonate derivatives of both half-molecules have the same chemical shifts yet are significantly broader than those for intact OTf (see Table I).

Experiments with Oxalate as the Synergistic Anion. When 1 equiv of Al^{3+} is added to apo-ovotransferrin in the presence of excess ^{13}C-labeled oxalate, three doublets (peaks e, f, and g) are observed in the carbonyl region of the ^{13}C NMR spectrum (Figure 5). The signals, upfield of free oxalate (a singlet at $\delta = 174.2$), increase in intensity when a second equivalent of the metal ion is added (especially peak f). The multiplet pattern is the result of two pairs of overlapping doublets (i.e., two AB spin systems), corresponding to the carboxyl carbons of oxalate bound to Al^{3+} through only one carboxylate group in both metal ion binding sites of OTf. ^{27}Al NMR spectra of the same experiments are shown in Figure 6. Upon addition of 1 equiv of metal ion, a signal at $\delta = -9.7$ (i, $\Delta\nu_{1/2} = 310$ Hz) is predominatly observed, plus another less intense signal at $\delta = -7.7$ (h, $\Delta\nu_{1/2} = 240$ Hz). When a second equivalent of Al^{3+} is added to the protein, the intensities of these resonances, in particular peak h, increase. The ^{27}Al signals are upfield of and significantly broader than those observed when carbonate serves as the synergistic anion. In the presence of excess Al^{3+}, signals due to the formation of a complex between oxalate and the metal ion emerge (^{13}C, $\delta = 166.2$; ^{27}Al, $\delta = 17$;[38] data not shown). As was the case for carbonate, these results suggest that in the presence of oxalate there is a preference for Al^{3+} binding at one site of OTf over the other; however, this site preference is not as pronounced under these conditions, since the binding is not completely sequential. The areas of both the ^{13}C and ^{27}Al NMR signals resulting from the complexation of Al^{3+} and oxalate at each site of OTf increase linearly with the addition of up to 2 equiv of metal ion, and no further changes are observed at higher concentrations of the metal ion (Figure 7). In this case, the protein is fully saturated with Al^{3+} at the end of the titration; this has been confirmed by simulations of ^{27}Al NMR spectra (i.e., the areas of peaks h and i in Figure 6c are approximately equivalent).

We have used the aluminum oxalate derivatives of the half-molecules of ovotransferrin to assign the signals diagnostic of Al^{3+} and $^{13}C_2O_4^{2-}$ binding to OTf discussed above (Figure 8). In the

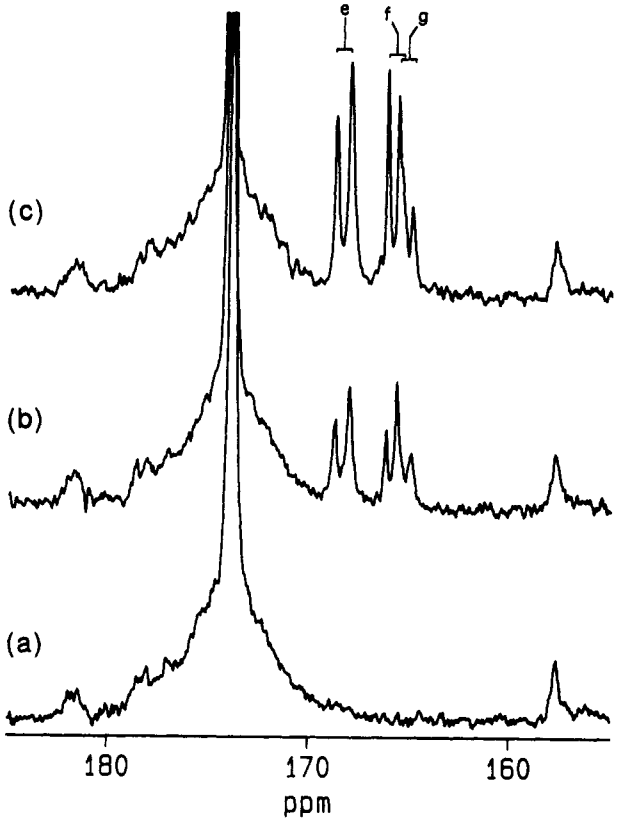

Figure 5. ^{13}C NMR spectra (100.6 MHz) of 1.18 mM OTf in the presence of 5 mM $Na_2{}^{13}C_2O_4$ and various amounts of Al^{3+} (pH 7.5, 20 000 scans each): (a) 0 equiv of Al^{3+}; (b) 1.0 equiv of Al^{3+}; (c) 2.0 equiv of Al^{3+}. Only the carbonyl region of each spectrum is shown.

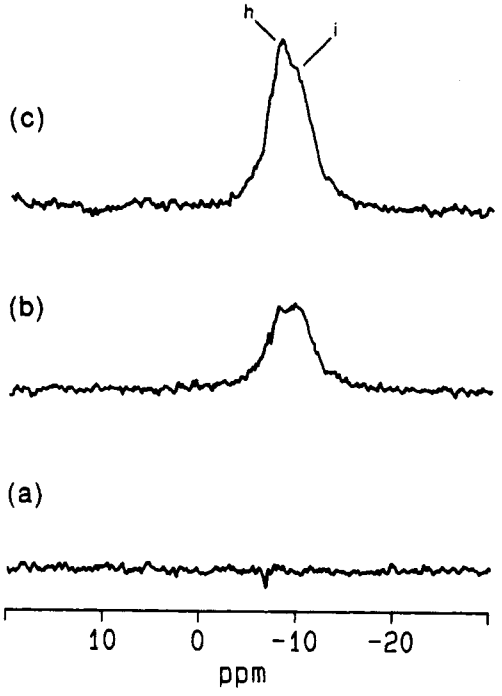

Figure 6. ^{27}Al NMR spectra (104.3 MHz) of 1.18 mM OTf in the presence of 5 mM $Na_2{}^{13}C_2O_4$ and various amounts of Al^{3+} (pH 7.5, 150 000 scans each): (a) 0 equiv of Al^{3+}; (b) 1.0 equiv of Al^{3+}; (c) 2.0 equiv of Al^{3+}.

(38) Jaber, M.; Bertin. F.; Thomas-David, G. *Can J. Chem.* **1977**, *55*, 3689–3699.

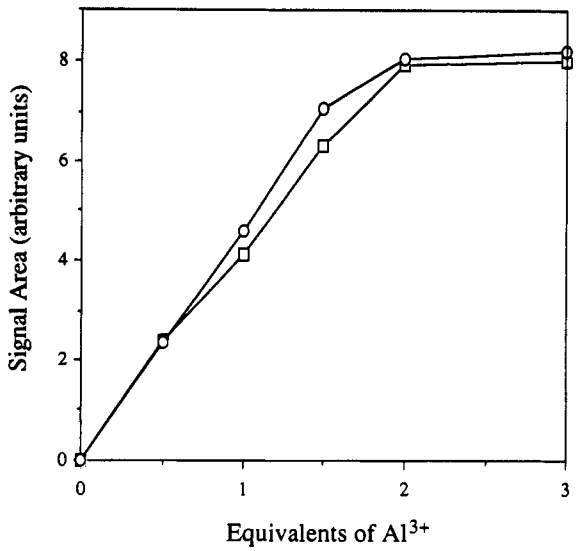

Figure 7. Dependence of the integrated signal areas of the ^{13}C (□) and ^{27}Al (○) NMR resonances corresponding to the binding of Al^{3+} to apo-OTf (1.18 mM, pH 7.5) in the presence of ^{13}C-labeled oxalate (5 mM) on the amount of metal ion added to the protein solution. For the ^{13}C data only, the area of peak e was used because of the emergence of a large signal in the same region as the upfield doublets at >2 equiv of Al^{3+} (see text). Again, at each point in the titration, both a ^{13}C and a ^{27}Al NMR spectrum were acquired (20 000 and 150 000 scans, respectively).

Table II. ^{13}C and ^{27}Al NMR Data for the Binding of Al^{3+} to OTf, OTf/2N, and OTf/2C in the Presence of ^{13}C-Labeled Oxalate[a]

(a) ^{13}C NMR

peak	δ	$^1J_{C-C}$ (Hz)[b]	assignment[b,c]	
e	168.47	73	Al^{3+}–O–C(O)–C(O)–O–	N
	168.42	70	Al^{3+}–O–C(O)–C(O)–O–	C
f	165.89	73	Al^{3+}–O–C(O)–C(O)–O–	N
g	165.33	70	Al^{3+}–O–C(O)–C(O)–O–	C

(b) ^{27}Al NMR

peak	δ	$\Delta\nu_{1/2}$ (Hz)	assignment[b]
h	−7.7	240	N-site
	(−4.4)	(170)	N-site
i	−9.7	310	C-site
	(−5.7)	(200)	C-site
OTf/2N	−7.8	480	
OTf/2C	−9.6	520	

[a] All ^{13}C data were acquired at a frequency of 100.6 MHz (9.4 T). The ^{27}Al data shown were obtained at frequencies of 104.3 MHz (9.4 T) and 130.3 MHz (11.7 T, in parentheses). [b] From ^{13}C NMR experiments on OTf/2N and OTf/2C; the ^{27}Al NMR assignments are also supported by the ^{27}Al chemical shifts for the half-molecules. [c] Assignment of the carboxyl carbons (underlined) in each site are as previously described.[10]

case of OTf/2C, two doublets which line up well with peaks e and g in the intact protein are clearly visible (Figure 8b). For OTf/2N, one again observes two doublets, this time corresponding to peaks e and f in the parent molecule. Interestingly, the downfield doublets resonate at slightly different frequencies in the half-molecules, and the spin–spin coupling constant, $^1J_{C-C}$, is slightly larger for oxalate bound to the N-site; see Table II for a complete list of the ^{13}C and ^{27}Al NMR signals and assignments from the aluminum oxalate experiments with OTf. For each site, the upfield doublet has been assigned to the carboxyl adjacent to the metal ion, whereas the high-frequency doublet corresponds to the carboxyl which interacts with residues in the binding cleft (see insets in Figure 8), on the basis of chemical shift data for several model compounds as previously described.[10] The half-molecule experiments also enable us to assign the ^{27}Al peaks (h and i) to bound Al^{3+} in the N- and C-terminal sites of the protein, respectively. Furthermore, from the titrations shown in Figures 5 and 6, it follows that Al^{3+} complexation occurs preferentially at the C-site of OTf when oxalate is present, in contrast to what is observed

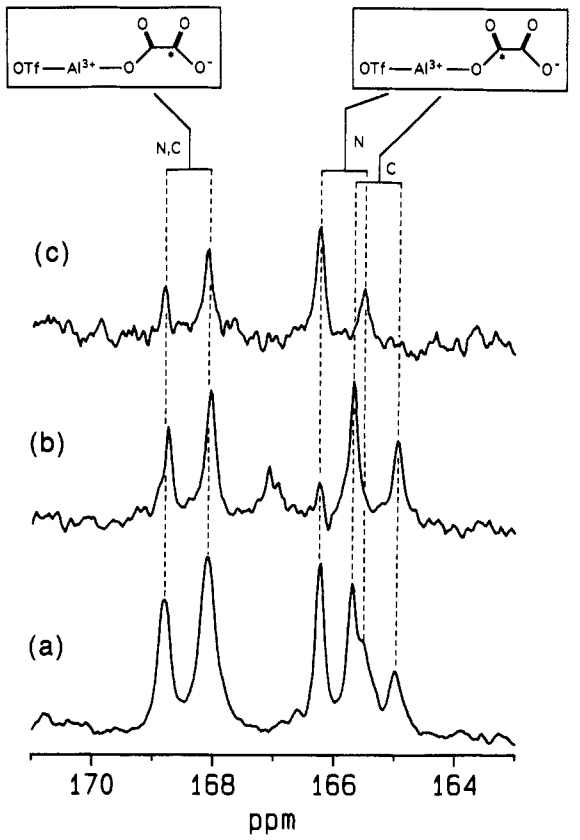

Figure 8. ^{13}C NMR spectra (100.6 MHz) of the aluminum oxalate derivatives of intact OTf and its half-molecules: (a) 1.18 mM OTf, 5 mM $Na_2{}^{13}C_2O_4$, 2 equiv of Al^{3+}, pH 7.5, 20 000 scans; (b) 0.72 mM OTf/2C, 2.5 mM $Na_2{}^{13}C_2O_4$, 1 equiv of Al^{3+}, pH 7.4, 40 000 scans; (c) 0.18 mM OTf/2N, 2.5 mM $Na_2{}^{13}C_2O_4$, 1 equiv of Al^{3+}, pH 7.7, 75 000 scans. Only a narrow window of the carbonyl region of each spectrum is shown. Peak assignments are shown in the insets. The peak at $\delta \approx 167$ ppm in spectrum b is an impurity that emerges in the preparation of OTf/2C after repeated recycling of this half-molecule.

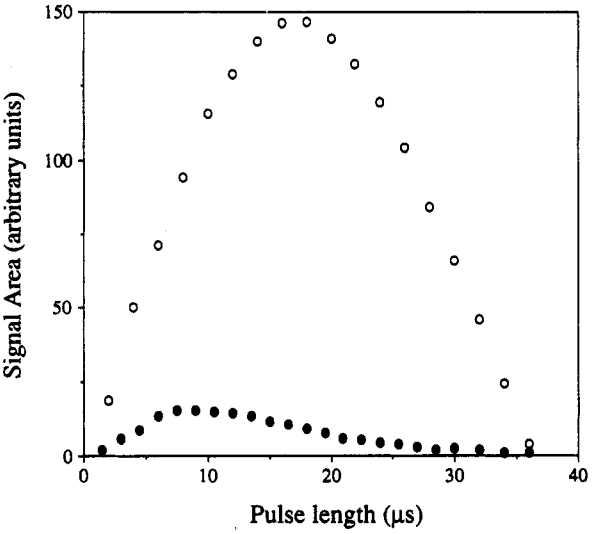

Figure 9. Dependence of the integrated ^{27}Al NMR (104.3 MHz) signal area of 1.00 mM $Al(NO_3)_3$ (○) and 1.00 mM (Al^{3+})-OTf-($^{13}CO_3{}^{2-}$) (●) on pulse length. A total of 50 000 scans were accumulated in each experiment, and a radio frequency pulse strength (ω_1) of 13.9 kHz was used throughout.

for carbonate. Again, the binding of Al^{3+} and oxalate by both half-molecules of OTf when monitored by ^{27}Al NMR showed the same chemical shifts and larger line widths for Al^{3+} bound to the proteolytic fragments compared to the parent molecule (see Table II).

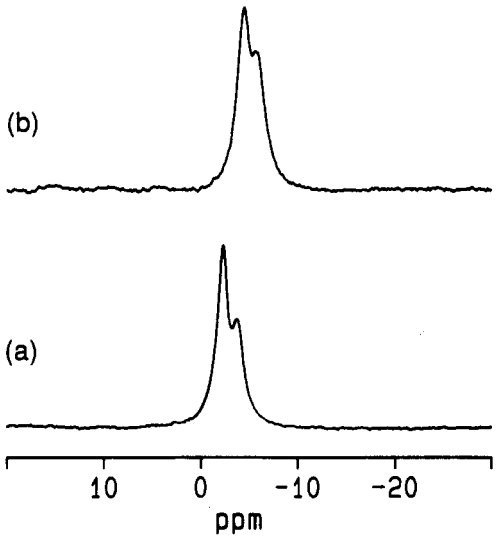

Figure 10. ^{27}Al NMR spectra (130.3 MHz) of the aluminum carbonate and aluminum oxalate derivatives of OTf at a magnetic field strength of 11.7 T: (a) 1.09 mM OTf, 20 mM $Na_2{}^{13}CO_3$, 2.0 equiv of Al^{3+}, pH 7.5, 100 000 scans; (b) 1.20 mM OTf, 5 mM $Na_2{}^{13}C_2O_4$, 2.0 equiv of Al^{3+}, pH 7.4, 100 000 scans.

Pulse Angle Dependence of OTf-Bound ^{27}Al NMR Signals. Plots of the integrated ^{27}Al signal areas from equimolar solutions of protein-bound and free aluminum (i.e., $Al(H_2O)_6^{3+}$) as a function of pulse length are shown in Figure 9. Two differences between the data for the metal ion in these environments are clearly noticeable. First, the area of the Al^{3+}-OTf signal attains its largest value at a pulse length ($\approx$8 μs) that is appreciably smaller than the 90° pulse for aqueous Al^{3+} (18 μs). Second, the area of the protein-bound ^{27}Al signal is significantly less than that observed for the free metal ion over virtually the entire spectrum of pulse lengths examined. In fact, the maximum area for the Al^{3+}-OTf signal was found to be only $\approx$18% of that from a spectrum of an equimolar aqueous solution of Al^{3+} acquired using the same flip angle ($\approx$40°). Virtually identical results were obtained for an equimolar solution of the aluminum oxalate derivative of OTf (data not shown).

Magnetic Field Dependence of OTf-Bound ^{27}Al NMR Signals. ^{27}Al NMR spectra (130.3 MHz) of OTf in the presence of 2 equiv of Al^{3+} and an excess of either carbonate or oxalate are shown in Figure 10. Increasing the external magnetic field from 9.4 to 11.7 T causes a decrease in line width and a 2–4-ppm downfield shift in peak position for each OTf-bound ^{27}Al signal (see Tables I and II). In both cases, the magnitude of these changes is larger for the signals due to bound Al^{3+} at the C-site. As a result, the resolution of the overlapping ^{27}Al peaks for both derivatives is only marginally improved (for comparison, see Figures 2c and 6c).

Discussion

The ^{13}C and ^{27}Al NMR studies of Al^{3+} binding to ovotransferrin and its half-molecules presented in this paper provide further spectroscopic evidence in favor of a difference in the two metal ion binding sites of this protein. In the presence of both carbonate and oxalate, two sets of peaks corresponding to the bound anion and metal ion in the two binding sites of the protein may be resolved by ^{13}C and ^{27}Al NMR. An initial ^{13}C NMR report of the dialuminum derivatives of sTf and OTf with these synergistic anions was presented some time ago by Bertini et al.[10] This group found a similar pattern of carbonyl signals for the oxalate experiment, in good agreement with our results. However, when carbonate was used only one broad resonance was observed for both proteins. We believe that this discrepancy with our findings stems from the fact that the closely spaced resonances resulting from carbonate binding at each site could not be resolved at the magnetic field strength used in the previous study. Preliminary investigations in our laboratory on human sTf and lTf have revealed that ^{13}C signals due to Al^{3+} and carbonate binding in the two sites of both proteins may also be resolved.[39]

In combination with the assignment information derived from the half-molecules of OTf, the Al^{3+} titration data illuminate some noteworthy differences in the behavior of the two sites when different synergistic anions participate in metal ion binding. In the presence of carbonate the N-terminal site of OTf has a significantly higher affinity for Al^{3+} than does the C-site. However, in the case of the larger oxalate anion, the specificity is reversed and the metal ion is preferentially bound to the C-site. The carbonate results are in agreement with a recent UV spectrophotometric study of Al^{3+} binding to OTf in which a ratio in the binding constants for this metal ion at the two sites (K_C/K_N) of 0.12 was reported, reflecting the site preference described above.[27] The exact opposite trend was demonstrated for human sTf,[26] suggesting an overall difference in the metal binding activities of these homologous proteins. In addition, our experiments indicate that OTf does not become fully saturated with Al^{3+} when carbonate acts as the synergistic anion, whereas with oxalate the titration is linear with the addition of up to 2 equiv of metal ion. A similar phenomenon has been demonstrated for the binding of Al^{3+} and carbonate to sTf, and it was proposed that competition from hydroxide ion (i.e., formation of $Al(OH)_3$) may account for this.[26] Ichimura et al. also reported that the binding of this metal ion to OTf shows negative cooperativity.[27]

The opposite site preferences for Al^{3+} binding to OTf in the presence of these two anions may be attributed to a difference in the ability of the sites to accommodate anions of different size. X-ray crystallographic studies of $(Fe^{3+})_2$-lTf-$(CO_3^{2-})_2$ and (Fe^{3+})-sTf/2N-(CO_3^{2-}) indicate that carbonate binds to Fe^{3+} in a bidentate fashion and fits snugly in a region between the metal ion and positively charged groups in the cleft.[17,21] On the basis of sequence homology and the fairly similar ionic radii of Al^{3+} and Fe^{3+} (0.54 and 0.65 Å, respectively[40]), an analogous situation may be predicted for the aluminum carbonate derivative of OTf. However, the volume of this anion binding site is insufficient to accommodate larger anions such as oxalate. It is thought, rather, that the second acidic moiety (i.e., a carboxylate) of such anions extends into a cavity beyond the anion binding site; this pocket may, in addition, participate in the binding of nonsynergistic ("secondary") anions such as chloride and perchlorate which can alter metal ion binding.[17] Our ^{13}C NMR results (in addition to those of Bertini et al.[10]) indicate that oxalate binds through only one carboxylate (probably in a bidentate fashion, like carbonate) to the metal ion and preferentially at the C-terminal site. This suggests that the C-terminal site of OTf is more adept at complexing anions that are larger than carbonate, thus modulating the affinity of the sites for Al^{3+}.

In general, in order to distinguish between the two iron binding sites in sTf and OTf, most researchers in the transferrin field have exploited the differences in the binding properties of the sites in these proteins to generate mixed derivatives with Fe^{3+} specifically loaded into one site of the protein and the metal ion of interest in the other.[41,42] The selectivity of iron binding in these proteins is dependent on a host of factors (i.e., pH, secondary anions), and we have experienced only mixed success using this technique for assignment purposes. In our opinion, the method of choice for assigning spectroscopic data of transferrins is the use of the half-molecules containing the intact sites. Methodologies for the synthesis of the half-molecules of both OTf and sTf by proteolytic digestion[32,43] and, recently, by expression have been described.[44] Our ^{13}C and ^{27}Al NMR results for the aluminum carbonate and aluminum oxalate derivatives of OTf/2N and OTf/2C clearly illustrate that mild proteolysis of intact OTf does not perturb the

(39) Aramini, J. M.; Vogel, H. J., unpublished results.
(40) Shannon, R. D. *Acta Crystallogr.* **1976**, *A32*, 751–767.
(41) Folajtar, D. A.; Chasteen, N. D. *J. Am. Chem. Soc.* **1982**, *104*, 5775–5780.
(42) Baldwin, D. A.; de Sousa, D. M. R. *Biochem. Biophys. Res. Commun.* **1981**, *99*, 1101–1107.
(43) Lineback-Zins, J.; Brew, K. *J. Biol. Chem.* **1980**, *255*, 708–713.
(44) Funk, W. D.; MacGillivray, R. T. A.; Mason, A. B.; Brown, S. A.; Woodworth, R. C. *Biochemistry* **1990**, *29*, 1654–1660.

structural integrity and metal ion binding activity of each lobe.

The ^{27}Al NMR spectra shown in this report represent, to our knowledge, the first successful attempts to directly monitor Al^{3+} binding to transferrins by NMR. Recently, Fatemi et al. failed to observe Al^{3+} bound to human sTf using this technique.[30] However, we feel that these workers may have missed the transferrin-bound ^{27}Al signal in their studies because they neglected to consider its marked pulse angle dependence (i.e., 90° pulses were used) and did not eliminate the broad and intense background aluminum signal. From numerous ^{27}Al NMR studies of low molecular weight inorganic aluminum complexes in recent years, it has been established that the ^{27}Al chemical shift range spans ≈300 ppm and that this parameter is indicative of the number of ligands involved in coordinating the metal ion.[28] The chemical shifts of the ^{27}Al signals due to OTf-bound Al^{3+} reported here fall well within a window ($\delta \approx 40$ to -46) that is diagnostic of six-coordinate (octahedral) Al^{3+} complexes.[28] This result is consistent with the recent X-ray structures of human lTf and rabbit sTf/2N.[17,21] In addition, the environment of bound Al^{3+} in the N-site of the protein appears to be more symmetric than that in the C-site on the basis of the consistently smaller line widths observed for the ^{27}Al signals corresponding to the metal ion in the N-site, regardless of the anion present. This may also account for the significantly narrower ^{27}Al signals observed when carbonate serves as the synergistic anion compared to oxalate (*vide infra*).

The peculiar properties of the OTf-bound ^{27}Al signals are characteristic of quadrupolar relaxation in a window of molecular motion that is well outside the extreme narrowing limit.[45-47] The first and, to our knowledge, only other observation in isotropic solution of these phenomena was presented by Butler and Eckert in an elegant ^{51}V NMR study of VO_2^+ binding to human sTf.[14] In general, for quadrupolar nuclei with half-integer spins ($I = {}^n/_2$, $n = 3, 5, 7, 9$), quadrupolar relaxation is described by the sum of $2I + 1$ exponentials, corresponding to the allowed single quantum transitions between the nuclear Zeeman levels. For $I = {}^5/_2$ nuclei such as ^{27}Al, these transitions may be grouped into three categories: I, ${}^1/_2 \rightarrow -{}^1/_2$; II, ${}^3/_2 \rightarrow {}^1/_2$ and $-{}^1/_2 \rightarrow -{}^3/_2$; III, ${}^5/_2 \rightarrow {}^3/_2$ and $-{}^3/_2 \rightarrow -{}^5/_2$. In the limit of fast molecular motion ($\omega_0\tau_c \ll 1$), the longitudinal and transverse relaxation rates ($1/T_1$ and $1/T_2$, respectively) of components I, II, and III are degenerate and one observes a single Lorentzian line. However, as $\omega_0\tau_c$ approaches a value of 1, this degeneracy is lost and the values of $1/T_2$ for the three components increase, resulting in broad non-Lorentzian signals. For motions that deviate substantially from extreme narrowing ($\omega_0\tau_c \gg 1$, as in the case of ^{27}Al bound to OTf[48]), the transverse relaxation rates of components II and III become extremely large, precluding their detection. However, the value of $1/T_2$ for component I actually decreases in this motional regime. Thus, the ^{27}Al signals detected for the aluminum carbonate and aluminum oxalate derivatives of OTf are almost entirely attributable to the central ${}^1/_2 \rightarrow -{}^1/_2$ transition. This accounts for the substantially lower integrated signal areas of OTf-bound Al^{3+}, which for small flip angles (i.e., up to ≈40°) is only 18–20% of that for the free metal ion and is comparable to the theoretically predicted limiting value (25.7%) of the contribution of component I to the signal area of an $I = {}^5/_2$ nucleus when $\omega_0\tau_c \gg 1$. In addition, the pulse angle dependence of a signal resulting from the central transition is predicted to be quite distinct from that observed under extreme narrowing conditions. In fact, in the limit of selective excitation of component I, the maximum intensity of the signal is expected to occur at a flip angle of $t_p/(I + {}^1/_2)$, where t_p is the 90° pulse length when all transitions are excited (i.e., 30° for ^{27}Al); this "flip angle effect" is a phenomenon that is not uncommon to solid-state NMR.[49,50] In our studies, the ^{27}Al signal area peaked at a pulse angle of ≈40° and no negative signals were observed up to a 180° flip angle, suggesting that components II and III may also be partially excited under these conditions.[14] Attenuating the power of the applied radio frequency pulse (ω_1) should increase the selectivity of the excitation of the central transition and, in principle, shift the effective 90° pulse length toward the predicted value.

Table III. Values of χ for the ^{27}Al NMR Signals Due to the Binding of Al^{3+} to OTf[a]

site	anion	$\Delta\delta_d$[b]	χ (MHz)
N	carbonate	2.3	3.4
C	carbonate	3.0	3.9
N	oxalate	3.3	4.1
C	oxalate	4.0	4.5

[a] Determined from the ^{27}Al chemical shift data for each signal at 9.4 and 11.7 T (see Tables I and II) using eq 1. [b] $\Delta\delta_d = \delta_{11.7\,T} - \delta_{9.4\,T}$.

Quadrupolar relaxation theory also accounts for a number of other interesting phenomena indicative of quadrupolar relaxation in the limit of slow molecular motion. For example, increasing $\omega_0\tau_c$ should result in a decrease in the transverse relaxation rate of component I and, hence, a decrease in the line width of the signal. Our results on the Al^{3+}-OTf species discussed in this paper at a field strength of 11.7 T confirm this prediction. Of course, one would expect a decrease in $\omega_0\tau_c$ to have the opposite effect, and this notion is substantiated by the increased line widths for the ^{27}Al signals of the half-molecules of OTf whose correlation times should be appreciably less than that of the intact protein ($\omega_0\tau_c \approx 65$ from the Stokes–Einstein equation.[48]). The chemical shift of component I is also affected by changes in the external magnetic field strength, a product of second-order dynamic frequency shifts.[51-53] We have found that increasing the field strength from 9.4 to 11.7 T results in a 2–4-ppm downfield shift in the positions of the OTf-bound ^{27}Al signals; the magnitude and direction of these shifts are in agreement with those observed for ^{51}V NMR signals of $V(V)_2$-sTf.[14] We have used this field-dependent chemical shift information to obtain estimates of the quadrupole coupling constant, χ, a parameter that is indicative of the symmetry of the ligand environment surrounding the metal nucleus. For very large values of $\omega_0\tau_c$, the dynamic frequency shift, $\Delta\omega_d$, approaches a constant value that is a function of only χ and ω_0; for a $I = {}^5/_2$ nucleus such as ^{27}Al, the shift is given by eq 1.[51] Since the ^{27}Al chemical shift data for the half-molecules

$$\Delta\omega_d = (6 \times 10^{-3})\left(\frac{\chi^2}{\omega_0}\right) \qquad (1)$$

are virtually identical to those of the intact protein in each case, this relation should hold. Using eq 1 and the ^{27}Al chemical shift data shown in Tables I and II, we have calculated values of χ for the four ^{27}Al signals observed in the Al^{3+} carbonate and Al^{3+} oxalate complexes of OTf (see Table III). The lowest values of χ are obtained when carbonate is the synergistic anion. Similarly, in the presence of either carbonate or oxalate, the value of χ for Al^{3+} bound to the N-site is less than that when bound to the C-site, suggesting a higher degree of symmetry about Al^{3+} in the N-terminal metal ion binding site. These trends are supported by

(45) Forsén, S.; Lindman, B. In *Methods of Biochemical Analysis*; Glick, D., Ed.; J. Wiley and Sons: New York, 1981; Vol. 27, pp 289–486.
(46) Bull, T. E.; Forsén, S.; Turner, D. L. *J. Chem. Phys.* **1979**, *70*, 3106–3111.
(47) Hubbard, P. S. *J. Chem. Phys.* **1970**, *53*, 985–987.
(48) The correlation time for human sTf has been estimated to be 2×10^{-7} s using the Stokes–Einstein equation $\tau_c = 4\pi\eta r^3/(3kT)$ and assuming that the molecule is a sphere with radius r (Koenig, S. H.; Schillinger, W. E. *J. Biol. Chem.* **1969**, *244*, 3283–3289). Using this value of τ_c for OTf and the resonance frequency of ^{27}Al at a magnetic field strength of 9.4 T (104.2 MHz), the value of $\omega_0\tau_c$ for OTf-bound ^{27}Al is approximately 130. In addition, by assuming an effective radius of $(0.5r^3)^{1/3}$ for each half-molecule (i.e. $0.79r$), rough estimates of τ_c (≈1×10^{-7} s) and $\omega_0\tau_c$ (≈65) for OTf/2N and OTf/2C may be obtained. In this discussion we are also assuming the absence of exchange between protein-bound and free Al^{3+}, a valid assumption in light of the high affinity that sTf exhibits for this metal ion ($K_D \approx 10^{-13}$ M; see ref 26 herein).
(49) Vega, S. *J. Chem. Phys.* **1978**, *68*, 5518–5527.
(50) Joseph, P. M.; Summers, R. M. *Magn. Reson. Med.* **1987**, *4*, 67–77.
(51) Drakenberg, T.; Forsén, S. In *The Multinuclear Approach to NMR Spectroscopy*; Lambert, J. B., Riddell, F. G., Eds.; D. Reidel: Dordrecht, 1983; pp 309–328.
(52) Westlund, P.-O.; Wennerström, H. *J. Magn. Reson.* **1982**, *50*, 451–466.
(53) Werbelow, L. G. *J. Chem. Phys.* **1979**, *70*, 5381–5383.

the line width data, as discussed above. It should also be possible to determine χ if the complete field dependence of each OTf-bound ^{27}Al signal is known; such work is currently in progress.

A number of studies have already shown that quadrupolar nuclei bound to small proteins may be monitored successfully by NMR spectroscopy. For example, the binding of Ca^{2+} to several calcium-binding proteins has been investigated using ^{43}Ca NMR.[54,55] This study demonstrates the feasibility of using ^{27}Al NMR to probe Al^{3+} binding to much larger proteins such as transferrins. In principle, this methodology may be extended to other metal-binding proteins and to other metal ions which have NMR-observable quadrupolar nuclei. However, as shown in this work and by Butler and Eckert,[14] the detectability of the central transition of quadrupolar nuclei bound to large proteins hinges considerably on a number of factors which are to some extent in the control of the experimentor and must be chosen with great care: (1) the strength of the external magnetic field (ω_0), (2) the size and motion of the macromolecule in question (τ_c, temperature, solution viscosity), (3) the intrinsic quadrupole moment of the specific nucleus (Q), and (4) the nature of the electric field gradient at the metal ion binding site.

(54) Vogel, H. J.; Forsén, S. In *Biological Magnetic Resonance*; Berliner, L. J., Reuben, J., Eds.; Plenum Press: New York, 1987; Vol. 7, pp 249-309.
(55) Aramini, J. M.; Drakenberg, T.; Hiraoki, T.; Ke, Y.; Nitta, K.; Vogel, H. J. *Biochemistry* **1992**, *31*, 6761-6768.

Acknowledgment. This research was supported by the Medical Research Council of Canada (MRC). The NMR spectrometers used in this work were purchased with funds provided by the MRC and the Alberta Heritage Foundation for Medical Research (AHFMR). J.M.A. is the recipient of a studentship from the Natural Sciences and Engineering Research Council of Canada (NSERC). H.J.V. is an AHFMR scholar.

Determination of the Nitrogen Chemical Structures in Petroleum Asphaltenes Using XANES Spectroscopy

Sudipa Mitra-Kirtley,[†,‡] Oliver C. Mullins,*[,†] Jan van Elp,[‡] Simon J. George,[§] Jie Chen,[‡] and Stephen P. Cramer[‡,§]

Contribution from Schlumberger-Doll Research, Ridgefield, Connecticut 06877, Lawrence Berkeley Laboratory, Berkeley, California 94720, and University of California, Davis, California 95616. *Received July 23, 1992*

Abstract: Extensive nitrogen K-edge X-ray absorption studies have been performed for the first time on seven petroleum asphaltenes and nitrogen standard compounds for the purpose of determining chemical forms of nitrogen present in the asphaltenes; such an objective is difficult to achieve by any other method. Sulfur XANES studies on fossil fuel samples have provided a rich source of information for the last ten years; similar XANES studies of nitrogen in fossil fuels have only recently been successfully performed using new, advanced fluorescence detection. Generally, the spectra of different chemical forms of nitrogen produce readily distinguishable features, thereby facilitating asphaltene analysis. Approximate contributions from different nitrogen structures present in the asphaltenes are calculated by comparing normalized areas under corresponding resonances in the spectra of the asphaltenes and the model compounds. The standard model compounds of nitrogen studied are pyrroles, pyridines, saturated amines, and metalloporphyrins. Most of the nitrogen in asphaltenes is found to be present in aromatic forms, with a very small amount as saturated amine. The pyrrole form of nitrogen is more abundant than the pyridine form in asphaltenes, and the pyridine fraction in different asphaltenes is somewhat variable. Pyridine, which is more basic than pyrrole, shows π^* resonances shifted to significantly lower energies than those observed for pyrroles. The relative positions of nitrogen π^* resonances are determined according to whether the nitrogen lone pair of electrons is shared in the π aromatic system. These spectral shifts are largely produced by resonance effects rather than inductive effects, which are observed in the sulfur case. Spectra of more complicated molecules such as porphyrins and imidazoles are explained along similar lines. The saturated amine shows only a σ^* resonance. Sensitivity of the spectra to surface effects is explored by comparing electron yield and fluoresence data.

Introduction

Asphaltenes are an important fraction of crude oil.[1] In the processing of crude oil, asphaltenes yield relatively small amounts of the most valuable hydrocarbon fractions. Asphaltenes often contain undesired heteroatoms such as sulfur and nitrogen and heavy metals such as nickel and vanadium which may poison catalysts. Physical properties of asphaltenes, such as solubility characteristics (which define asphaltenes), are important. In the production of crude oil, maintenance of formation pressures by injection of gases such as CH_4 and CO_2 can result in the in situ precipitation of asphaltenes, thereby resulting in the reduction of formation permeability. Knowledge of the chemical structures of asphaltenes is important for the optimal production and processing of crude oils. Here we use X-ray absorption near-edge structure (XANES) spectroscopy to investigate the different structural forms of nitrogen in asphaltenes.

Asphaltenes, the heaviest component of petroleum, are dark brown or black infusible solids. They are dispersed in crude oil by association with the resins, probably in a micelle structure. Asphaltenes are defined by their solubility characteristics instead of their chemical classification;[1-3] they are insoluble in light hydrocarbons, such as *n*-heptane, but soluble in more polarizable solvents, such as benzene. Heteroatom constituents of asphaltenes play an important role in determining the solubility characteristics. In spite of their varied sources, asphaltenes generally exhibit many invariant chemical properties. Asphaltenes consist of complex macromolecules, composed principally of condensed aromatic nuclei with substituted alkyl and alicyclic systems.[1-3] The mo-

[†] Schlumberger-Doll Research.
[‡] Lawrence Berkeley Laboratory.
[§] University of California, Davis.

(1) *Chemistry of Asphaltenes*; Bunger, J. W., Li, N. C., Eds.; American Chemical Society: Washington DC, 1981.
(2) *Bitumens, Asphalts and Tar Sands*; Chillingarian, G. V., Yen, T. F., Eds.; Elsevier Scientific Pub. Co.: New York, 1978.
(3) Speight, J. G. *The Chemistry and Technology of Petroleum*; Marcel Dekker, Inc.: New York, 1980.

0002-7863/93/1515-252$04.00/0